Automatic Calculation of Disc Foveal-Angle

Mona A. Mohammed, Nancy M. Salem, Mohamed El Dosoky

Abstract— Strabismus refers to a condition in which eyes are misaligned. Proper alignment of eyes is important to avoid seeing double, to experience good depth perception and to prevent developmental or learning delays and consequences of anxiety. The earlier the treatment, the better the results, it may be caused by overactive or underactive eye muscles. The position of the fovea with respect to the optic disc (OD) is used to identify whether the image is normal or abnormal ocular torsion (Extorsion or Intorsion). In this paper, a method for automatic Disc Foveal-Angle (DFA) calculation to detect the type of ocular torsion is proposed. First step for DFA calculation is the OD localization by using the Canny edge detector followed by a circular Hough transform. Second step is to localize the fovea, where the Wellner`s adaptive threshold is used followed by Canny edge detector and circular Hough transform. A set of 1250 fundus images are used from two publicly available datasets (DRIVE and MESSIDOR) in addition to a local dataset. Results show that this method is reliable and accurate for the DFA calculation and for the detection of the ocular type.

Index Terms— DFA, Optic disc localization, Fovea localization, Extorsion, Intorsion.

1 Introduction

According to the National Eye Institute, strabismus affects approximately 1 in every 25 to 50 individuals in the US (2-4% of the population). This also translates into approximately 6 to 12 million people in the US. Worldwide, this would estimate to anywhere between 130 to 260 million people [1].

Extorsion and intorsion are types of strabismus. Ocular torsion was measured in multiple ways, most usually subjectively, with double Maddox rods or, rarely, with the Lancaster Red-Green Test. Objectively, there were additional measurement techniques: blind spot mapping, fundus images, and estimation by indirect ophthalmoscopy [2].

Many advantages for the double Maddox rod test as it is easy to perform, it is quickly completed, and it provides a quantitative measurement of subjective torsion. In the double Maddox rod test the patient fixates on a point source of light while two Maddox rod lenses, usually one red and one white Maddox rod, are placed in front of each eye to produce two horizontal lines. A patient with normal subjective torsion will see two parallel horizontal lines. If an eye has abnormal torsion, the lines will not appear parallel. The patient is guided to rotate the appropriate Maddox rod lenses until the lines become horizontal and parallel. The degree of subjective torsion matches the final position of the Maddox rods [2].

In the literature, DFA is an important primary step before and after weakening surgery of the superior oblique muscle [3], [4], measurement of normal ocular torsion [5], and the evaluation of the hypertropia and excyclotorsion [6]. Accurate calculation for the DFA enhances the performance of retinal nerve fiber layer (RNFL) measures for glaucoma detection, where knowledge of the normal RNFL thickness profile is important in detecting and following patients with glaucoma [7]. Another application of DFA is to assess an objective fundus torsion evaluation in pediatric population with using Non-Mydriatic Fundus Photography (NMFP) in healthy and cyclovertical strabismus patients to evaluate the DFA over time and observers [8].

Recently, there are many work proposed in the literature for calculating the DFA from Optical Coherence Tomography (OCT) [7], or from color fundus images [3], [4], [5], [6], [8], [9].

In the work reported in [3], the torsion angle is measured using AutoCAD 2009(R) by creating a tangent rectangle of four sides for the OD . This was the way to identify the center of the OD. Then, other line was sketched linking the center of the OD to the center of the fovea, and the DFA angle was calculated.

In the work reported in [4], [5], the torsion angle is measured from the print using a protractor. In [6], A connecting line between the center of the optic disc and the fovea, and the another line was sketched horizontally from the fovea, and the DFA was expressed in idioms of tangential value.

In the work proposed in [8], three main marks were chosen on the pictures that recorder for the patient to determine the DFA. The marks are: the center of the fovea, the top edge, and the bottom border of the OD. The Adobe Photoshop Elements software is used to determine the DFA angle between the middle of the disc, the fovea and the horizontal line traversing it. On the other hand, the PowerPoint (Microsoft Corp, Redmond, WA) is used to measure the DFA in [9].

A semi-automated technique for estimating the DFA from SD-OCT machine images is proposed in [7]. The center of fovea is identified automatically by Matlab but the center of OD is identified by two methods, the first method is done by OCT automated algorithm but it wasn`t accurate method so by using the least-square method which is semi-automated the OD center was identified.

- *Mona A. Mohammed is a biomedical ngineer in Research Institute of Ophtholomology, Cairo, Egypt. E-mail: Eng.m737@gmail.com*
- *Nancy M. Salem is associate professor in Faculty of Engineering, Biomedical Engineering Department, HELWAN University, Cairo, Egypt.E-mail: nancy_salem@h-eng.helwan.edu.eg*
- *Mohamed Eldosoky is professor in Faculty of Engineering, Biomedical Engineering Department, HELWAN University, Cairo, Egypt.*

2 METHODOLOGY

The proposed DFA calculation algorithm and classification of the torsion type are explained in the next sub-sections. DFA calculation algorithm involves two steps including OD localization and fovea localization. Then, detecting the type of torsion will be based on the position of the fovea with respect to the OD.

2.1 Optic Disc Localization

In this sub-section, a method to locate and detect the center of the OD.

2.1.1 Fundus image pre-processing

Pre-processing is proceeded in order to detect the abnormalities, correct the uneven illumination and remove the unwanted pixels present in the input fundus image [10]. The color RGB fundus image is converted to an intensity image to combine information from red and green channels [11]. As the OD is located either on the left or right side of the fundus image; pre-processing involves identifying the half that contains the OD by segmenting the vascular tree and finding the half with brighter objects.

Then, blood vessel are eliminated to facilitate the segmentation of the OD and to increase the segmentation accuracy. These steps are shown in Fig. 1 (a, b and c).

2.1.2 Identifying the Center of OD

To identify the center of OD, the image is smoothed using Gaussian filter followed by the Canny edge detector. Finally, the circular Hough transform is applied to detect the circular region that represents the OD. These steps are shown in Fig. 1 (d, e, and f).

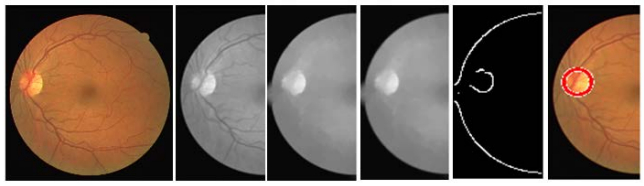

(a) (b) (c) (d) (e) (f)

Fig. 1. (a) RGB fundus image, (b) Intensity half that contains OD, (c) Blood vessels elimination, (d) Filtered image, (e) Canny edge detector, and (f) Circular Hough transform.

The Hough transform can be used for representing objects that can be parameterized mathematically. The circle can be parameterized in Eqn. 1:

$$(x - a)^2 + (y - b)^2 + r^2 = 0 \qquad (1)$$

Where (a, b) is the coordinate of the center of the circle that passes through (x, y) and r is its radius. The OD and its center are detected as shown in Fig. 2.

Fig. 2. Identification of the center of OD.

2.2 Fovea Localization

To identify the center of fovea, processing involves three steps including Wellner's adaptive threshold [10], Canny edge detector, and Circular Hough transform [12], [13]. First, Wellner's adaptive thresholding algorithm is applied to the intensity image. Then, Canny edge detector is used to segment the fovea. Finally, the circular Hough transform can identify center of fovea. These steps are shown in Fig. 3.

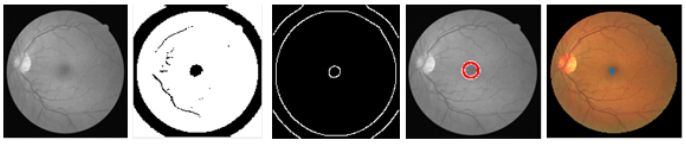

(a) (b) (c) (d) (e)

Fig. 3. Image after: (a) Intensity transformation, (b) Wellner's adaptive threshold, (c) Canny edge detector, (d) Fovea localization, and (e) Identifying the center of fovea.

2.3 DFA Calculation

The DFA is the angel between the lines AB and AC. Where, AB is a horizontal line passing through point A (the center of the OD). AC is the line passing through the centers of the fovea and the optic disc as illustrated in Fig. 4.

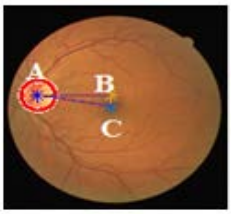

Fig. 4. Disc foveal angle.

2.4 Ocular Torsion Detection

One of the clinical applications of OD and fovea localization is the detection of the type of ocular torsion. The normal range for the fovea is within the lower third of the optic disc (in the view of fundus images). There are two types of abnormal ocular torsion: intorsion and extorsion, as shown in Fig. 5 as reported in [8].

3 Experimental Results

The proposed algorithm is implemented using Matlab R2016a on a PC with an Intel(R) Core (TM) i3 and 6 GB RAM.

3.1 Datasets

The DRIVE dataset of retinal images: contains 40 fundus images of dimensions 584×565 pixels (33 normal and 7 diseased) with field of view 45° and with images format TIFF for blood vessels ground truth [14].

The MESSIDOR dataset of retinal images: consists of 1200 fundus images of dimensions 1440×960, 2240×1488 or 2304×1536 pixels with field of view 45° and with images format TIFF, images were acquired by 3 ophthalmologic departments using a color video 3CCD camera on a Topcon TRC NW6 non-mydriatic retinograph [15].

The local dataset of retinal images: consists of 10 fundus images of dimensions 2336×1833 and with images format JPG. Images were acquired by a color video camera on a Topcon TRC 50DX non-mydriatic retinograph.

Figure 6 shows sample results for the OD and fovea localization.

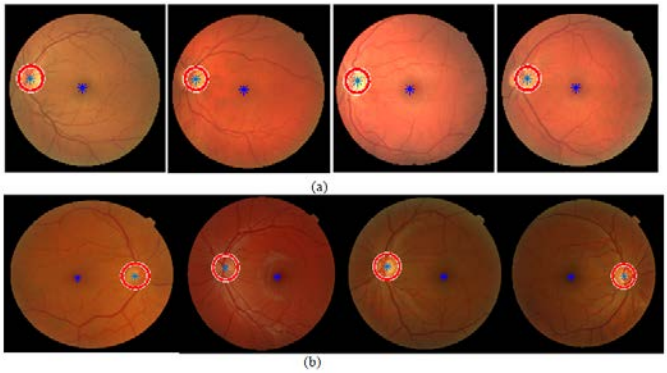

Fig. 6. OD and fovea Localization for images from (a) DRIVE dataset and (b) MESSIDOR dataset.

3.2 Result and Discussions

For the DRIVE dataset, the proposed algorithm correctly localize the optic disc in 40 images with a success rate of 100%, and localize the fovea in 35 images out of 40 images (5 images have been excluded for not having visually-detectable fovea). This results in a set of 35 images to be used in the DFA calculations.

For the MESSIDOR dataset, a set of 1200 images were used for performance evaluation. The proposed algorithm correctly localize the optic disc in 1195 images with a success rate of 99.6%, and localize the fovea in 1196 images out of 1200 (3 images have been excluded for not having visually-detectable fovea) images. This results in a set of 1188 images to be used in the DFA calculations.

For the Local dataset, the proposed algorithm correctly localize the optic disc in 10 images with a success rate of 100%, and localize the fovea in 10 images out of 10 images. This results in a set of 10 images to be used in the DFA calculations.

Results for OD and fovea localization are summarized in Tables 1 and 2. Table 3 summarizes results for DFA.

A Comparison between OD detection methods from the literature [10], [16], [17], [18], [19], [20] and the proposed method is summarized in Table 4. Another comparison between fovea detection methods from the literature [10], [21], [22], [23], [24], [25] and the proposed method is summarized in Table 5.

TABLE 1
RESULTS FOR OD LOCALIZATION

Dataset	Tested images	OD localization	Success rate
DRIVE	40	40	100%
MESSIDOR	1200	1195	99.583%
Local	10	10	100%

TABLE 2
RESULTS FOR FOVEA LOCALIZATION

Dataset	Tested images	Eliminated images (not having visually-detectable fovea)	Fovea localization failed	Fovea localization	Success rate
DRIVE	40	5	0	35	100%
MESSIDOR	1200	3	1	1196	99.916%
Local	10	0	0	10	100%

TABLE 3
RESULT FOR DFA CALCULATION

Dataset	Tested images	Miss identified center of OD	Miss Identified center of fovea	Miss identified center for both OD and fovea	DFA calculated
DRIVE	40	1	5	1	35
MESSIDOR	1200	8	4	0	1188
Local	10	0	0	0	10

TABLE 4

COMPARISON BETWEEN OD DETECTION METHODS AND THE PROPOSED METHOD

Method	Success Rate	
	Drive dataset	MESSIDOR dataset
E. Nandhini et al. [10]	--------	99.44% (540 healthy images) 99.24% (660 pathological images)
D. A. Godse et al. [16]	100%	--------
M. K. Aggarwal et al. [17]	95%	--------
H. Ullaha et al. [18]	100%	--------
A. Dehghani et al. [19]	100%	--------
K. Yaseen et al. [20]	Hough: 100% Log: 85%	--------
Proposed method	100%	99.583% (1200 images)

TABLE 5

COMPARISON BETWEEN FOVEA DETECTION METHODS AND THE PROPOSED METHOD

Method	Success Rate	
	Drive dataset	MESSIDOR dataset
E. Nandhini et al. [10]	--------	99.62% (540 healthy images) 98.93% (660 pathological images)
K. S. Chin et al. [21]	--------	80% images with no risk of macula edema 59% images with risk of macula edema (303 retinal images)
L. Kovacs et al. [22]	89.3% (40 images)	--------
D. Deka et al. [23]	100% (36 images)	97.75% (800 images)
S. Onal et al. [24]	--------	97.4% (1200 images)
K. M. Asim et al. [25]	100% (40 images)	--------
Proposed method	100% (40 images)	99.919% (1200 images)

Figure 7 shows the calculation of the DFA for a set of sample images. To detect the type of ocular torsion, the center of the fovea is located with respect to the lower third of the OD as:

- If fovea is located within the lower third of the OD as shown in Fig. 8(a), neither extorsion nor intorsion are present.
- If fovea is located below the lower third of the OD as shown in Fig. 8(b), then extortion is present.
- If fovea is located upper than the lower third of the OD as shown in Fig. 8(c), then intortion is present.

Results for the detection the type of ocular torsion for 35 images from the DRIVE dataset, 1188 images from MESSIDOR dataset and 10 images from the Research Instituite of Ophtholmology are summarized in Table 6.

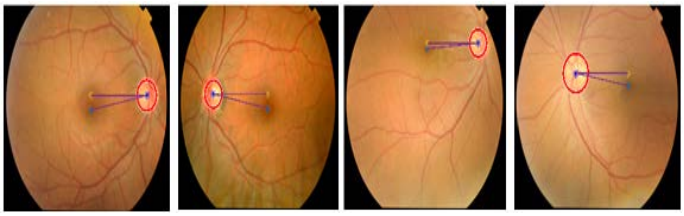

DFA= -9.2981° DFA= -9.1797° DFA = -3.7852° DFA = -8.7571°

Fig. 7. DFA calculations.

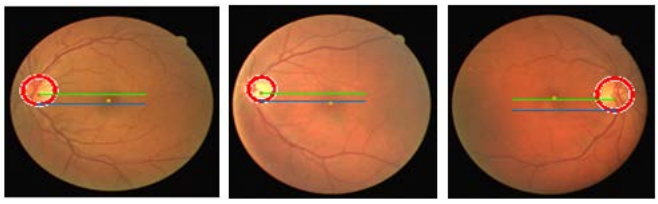

(a) (b) (c)

Fig. 8. (a) Normal ocular torsion, (b) Extorsion, and (c) Intorsion.

TABLE 6

DETECTION OF THE TYPE OF THE OCULAR TORSION

Dataset	Tested images	Type of Ocular Torsion		
		Normal	Intorsion	Extorsion
DRIVE	35	24	6	5
MESSIDOR	1188	836	221	131
Local	10	7	1	2

For performance evaluation, the DFA calculated from the proposed method (for the DRIVE dataset) have been checked and approved by an expert. The type of ocular torsion has been correctly classified as either intorsion or extorsion. The Double Maddox Rod Test has been used to evaluate the results for the local dataset (10 images).

4 Conclusion

In this paper, a method to calculate the DFA and to determine the type of ocular torsion from color fundus images is proposed. To calculate the DFA, the OD and fovea are localized using image processing techniques. The position of the fovea with respect to the OD is used to identify the type of ocular torsion as extorsion or intorsion. Images from three different datasets have been used for performance evaluation. This method can be used as a computer aided diagnosis tool to follow-up patients by calculating the DFA before and after ocular surgeries.

References

[1] *The Center for Visual Management*. Available: http://www.thecenterforvisualmanagement.com/strabismus.html?fbclid=IwAR3H5PQyNx1TsCnOkYa53D6QhQE4YSfzhhTryRGTa9SYVdYT5tmcZgzeadI.

[2] A. L. Rosenbaum and A. P. Santiago, *Clinical strabismus management: principles and surgical techniques*: David Hunter, 1999.

[3] B. L. Ducca, C. R. d. Souza-Dias, A. C. F. Lui, and M. Goldchmit, "Measurement of ocular torsion variation following superior oblique tenectomy," *Arquivos brasileiros de oftalmologia,* vol. 77, pp. 364-367, 2014.

[4] P. Sharma, S. Thanikachalam, S. Kedar, and R. Bhola, "Evaluation of subjective and objective cyclodeviation following oblique muscle weakening procedures," *Indian journal of ophthalmology,* vol. 56, pp. 39-43, 2008.

[5] J. Jethani, G. Seethapathy, J. Purohit, and D. Shah, "Measuring normal ocular torsion and its variation by fundus photography in children between 5-15 years of age," *Indian journal of ophthalmology,* vol. 58, pp. 417-419, 2010.

[6] J. J. Lee, K. I. Chun, S.-H. Baek, and U. S. Kim, "Relationship of hypertropia and excyclotorsion in superior oblique palsy," *Korean Journal of Ophthalmology,* vol. 27, pp. 39-43, 2013.

[7] N. Amini, S. Nowroozizadeh, N. Cirineo, S. Henry, T. Chang, T. Chou, *et al.*, "Influence of the disc–fovea angle on limits of rnfl variability and glaucoma discrimination," *Investigative ophthalmology & visual science,* vol. 55, pp. 7332-7342, 2014.

[8] C. Le Jeune, F. Chebli, L. Leon, E. Anthoine, M. Weber, A. Péchereau, *et al.*, "Reliability and reproducibility of disc-foveal angle measurements by non-mydriatic fundus photography," *PloS one,* vol. 13, pp. 1-9, 2018.

[9] J. Jethani and P. Dave, "A technique for standardizing disk foveal angle measurement," *Journal of American Association for Pediatric Ophthalmology and Strabismus,* vol. 19, pp. 77-78, 2015.

[10] E. Nandhini and S. R. Malathi, "Location of fovea centralis in digital fundus images using adaptive thresholding method," *International Journal of Pharma and Bio Sciences,* vol. 5, pp. 590 - 600, 2014.

[11] F. A. Hashim, N. M. Salem, and A. F. Seddik, "Automatic segmentation of optic disc from color fundus images," *Jokull Journal,* vol. 63, pp. 142-153, 2013.

[12] V. Patil, V. Kumbhakarna, and S. Kawathekar, "Detection of Optic Disc in Retina Using Hough Transform," *INTERNATIONAL JOURNAL OF COMPUTERS & TECHNOLOGY,* vol. 15, pp. 6613-6617, 2016.

[13] V. Thongnuch and B. Uyyanonvara, "Automatic detection of optic disc from fundus images of ROP infant using 2D circular hough transform," *Sirindhorn International Institute of Technology, Thammasat University, Thailand,* 2006.

[14] J. Staal, M. D. Abràmoff, M. Niemeijer, M. A. Viergever, and B. Van Ginneken, "Ridge-based vessel segmentation in color images of the retina," *IEEE transactions on medical imaging,* vol. 23, pp. 501-509, 2004.

[15] E. Decencière, X. Zhang, G. Cazuguel, B. Lay, B. Cochener, C. Trone, *et al.*, "Feedback on a publicly distributed image database: the Messidor database," *Image Analysis & Stereology,* vol. 33, pp. 231-234, 2014.

[16] D. A. Godse and D. S. Bormane, "Automated localization of optic disc in retinal images," *International Journal of Advanced Computer Science and Applications,* vol. 4, pp. 65-71, 2013.

[17] M. K. Aggarwal and V. Khare, "A new method for optic disc localization in retinal images," in *2016 Ninth International Conference on Contemporary Computing (IC3)*, 2016, pp. 1-5.

[18] H. Ullaha, N. Islam, Z. Jan, H. Farman, B. Jan, G. Jeon, *et al.*, "Optic disc segmentation and classification in color fundus images: a resource-aware healthcare service in smart cities," *Journal of Ambient Intelligence and Humanized Computing,* pp. 1-13, 2018.

[19] A. Dehghani, H. A. Moghaddam, and M.-S. Moin, "Optic disc localization in retinal images using histogram matching," *EURASIP Journal on Image and Video Processing,* vol. 2012, p. 19, 2012.

[20] K. Yaseen, A. Tariq, and M. U. Akram, "A Comparison and Evaluation of Computerized Methods for OD Localization and Detection in Retinal Images," *International Journal of Future Computer and Communication,* vol. 2, pp. 613-616, 2013.

[21] K. S. Chin, E. Trucco, L. Tan, and P. J. Wilson, "Automatic fovea location in retinal images using anatomical priors and vessel density," *Pattern Recognition Letters,* vol. 34, pp. 1152-1158, 2013.

[22] L. Kovacs, R. J. Qureshi, B. Nagy, B. Harangi, and A. Hajdu, "Graph based detection of optic disc and fovea in retinal images," in *4th International Workshop on Soft Computing Applications*, 2010, pp. 143-148.

[23] D. Deka, J. P. Medhi, and S. Nirmala, "Detection of macula and fovea for disease analysis in color fundus images," in *2015 IEEE 2nd International Conference on Recent Trends in Information Systems (ReTIS)*, 2015, pp. 231-236.

[24] S. Onal, X. Chen, V. Satamraju, M. Balasooriya, and H. Dabil-Karacal, "Automated and simultaneous fovea center localization and macula segmentation using the new dynamic identification and classification of edges model," *Journal of Medical Imaging,* vol. 3, p. 034002, 2016.

[25] K. M. Asim, A. Basit, and A. Jalil, "Detection and localization of fovea in human retinal fundus images," in *2012 International Conference on Emerging Technologies*, 2012, pp. 1-5.